Journal of Materials Chemistry A

PAPER

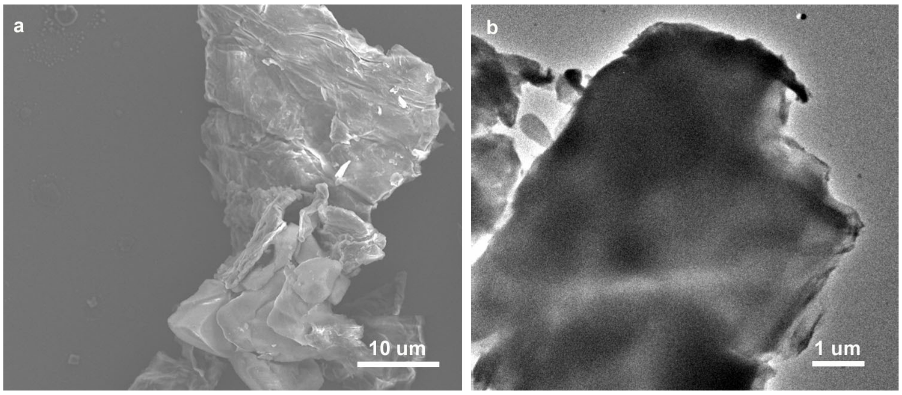

Figure S1. a-b SEM and TEM images of graphite oxide powder.

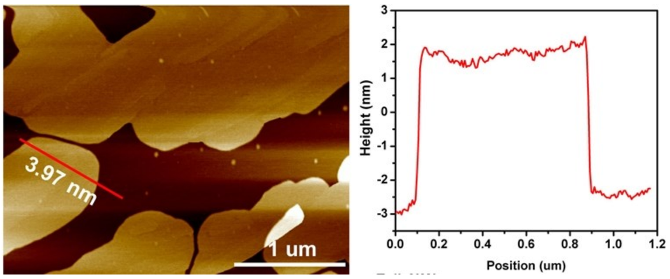

Figure S2. AFM image of tert-GO.

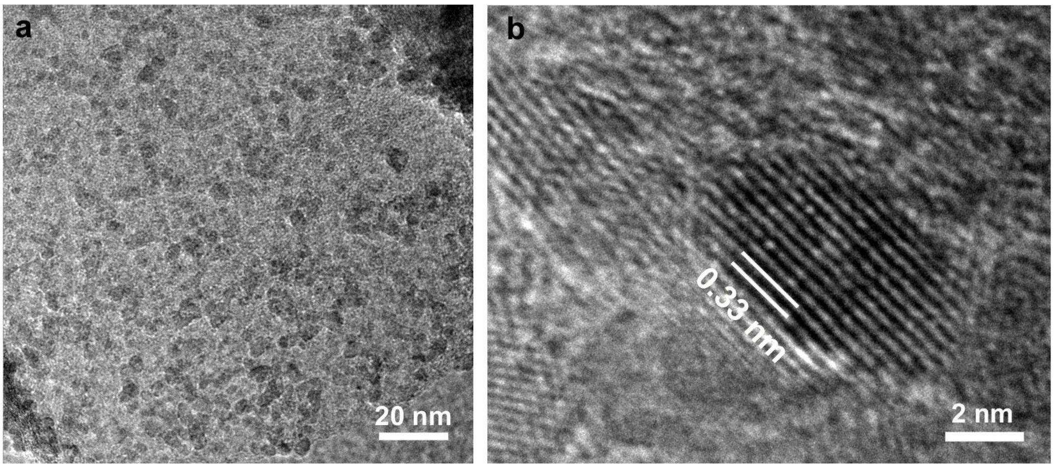

Figure S3. a TEM image of SnO_2 /tert-GO catalysts. b A higher magnification STEM image of SnO_2 /tert-GO.

Please do not adjust margins

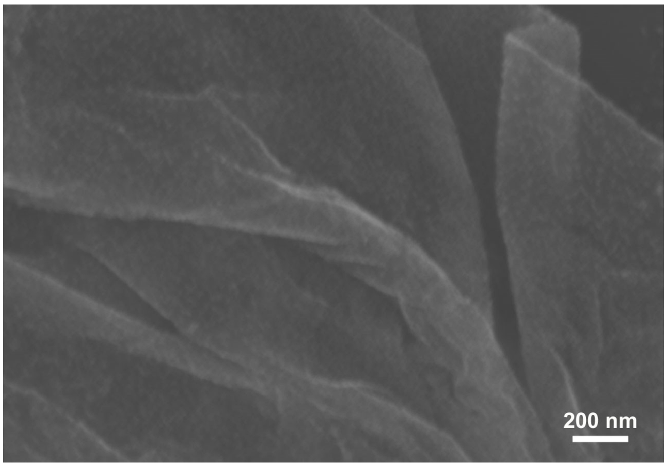

Figure S4. SEM image of SnO_2/tert-GO.

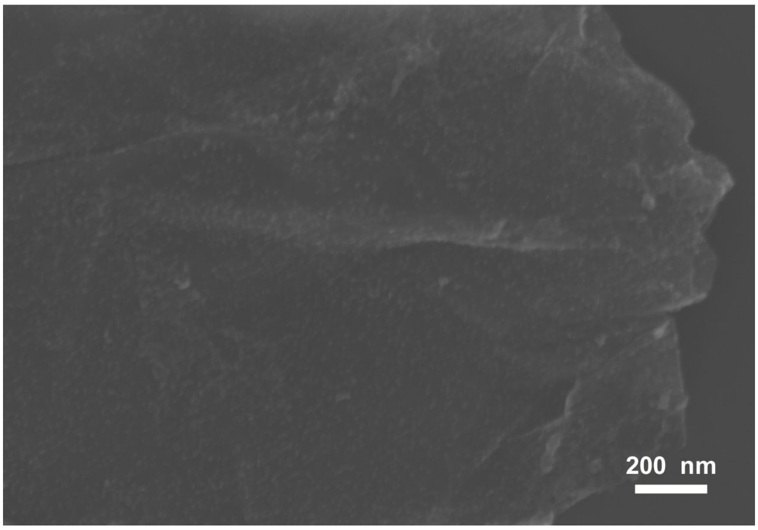

Figure S5. SEM image of SnO_2/GO.

Please do not adjust margins

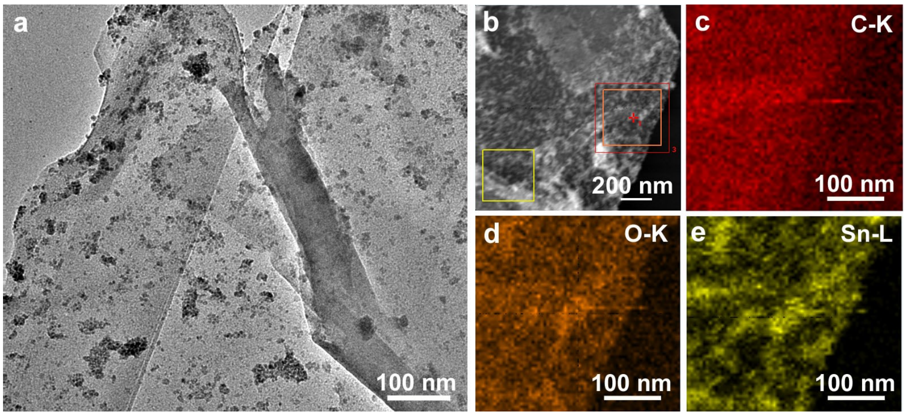

Figure S6 a TEM bright-field image of SnO_2/GO catalysts. b A higher magnification STEM image of SnO_2/GO catalysts. c-e the X-EDS mappings of SnO_2/GO catalysts.

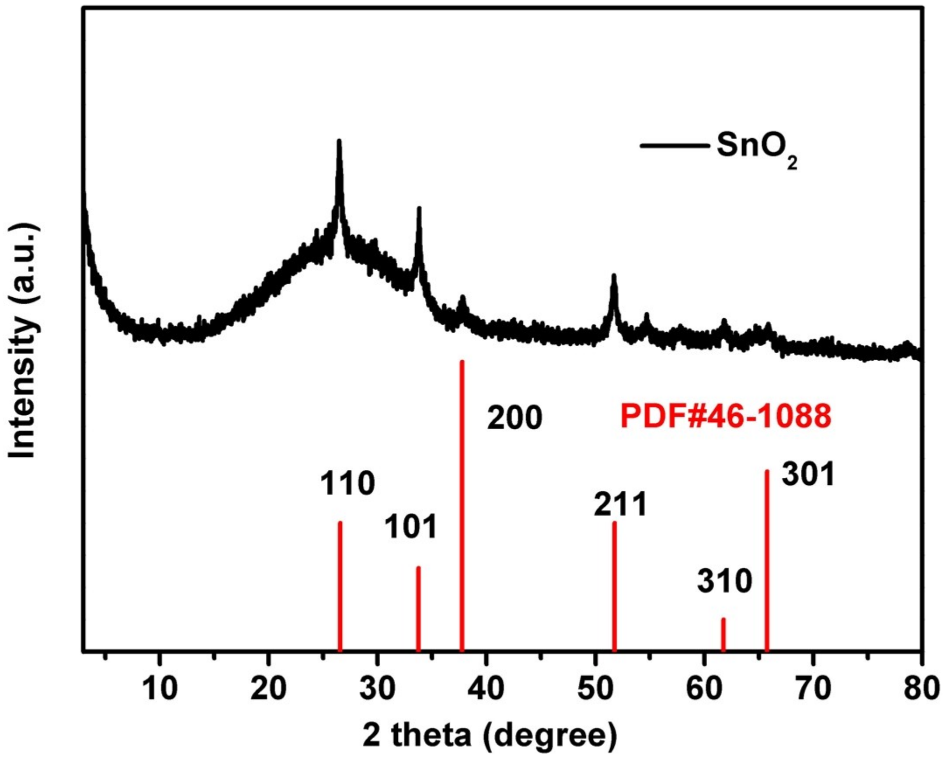

Figure S7. XRD pattern of SnO_2 catalyst.

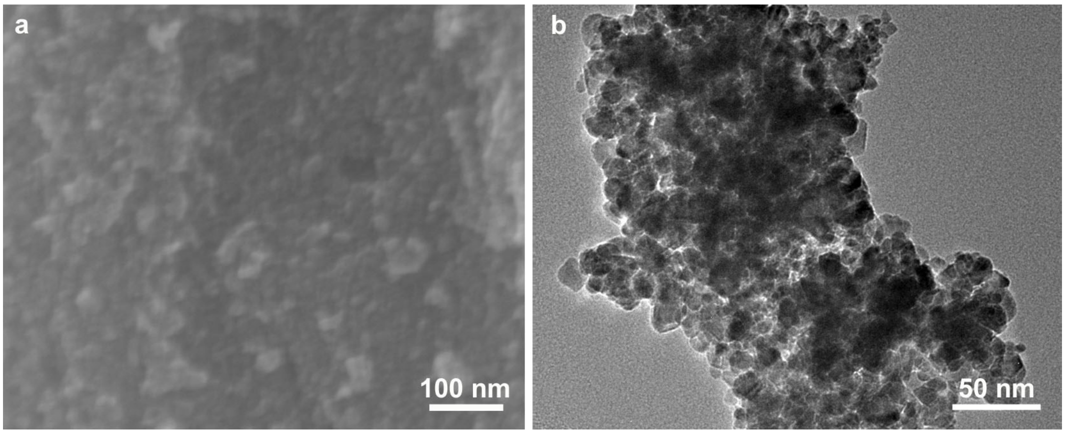

Figure S8. a-b SEM and TEM images of SnO_2.

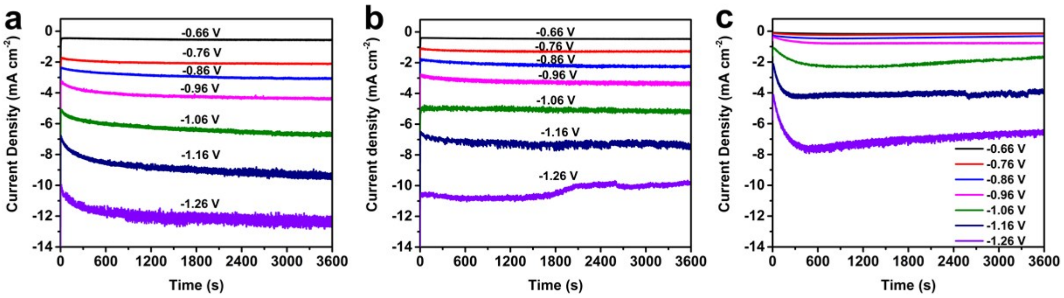

Figure S9. a-c Chronoamperometric curves of SnO_2/tert-GO, SnO_2/GO and SnO_2 at different applied potentials as indicated.

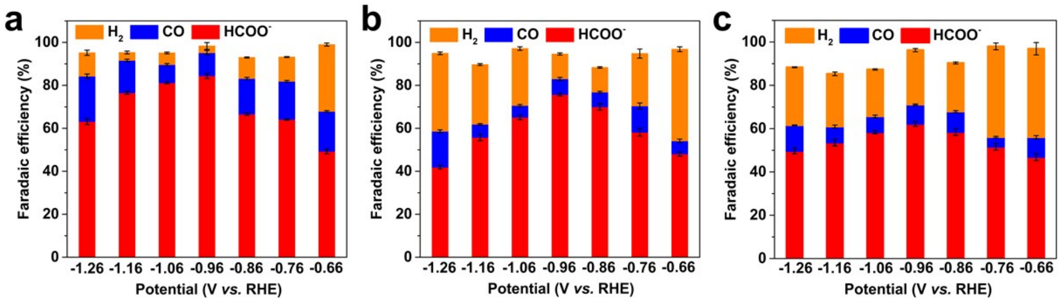

Figure S10. a-c $HCOO^-$, CO and H_2 Faradaic efficiency for SnO_2/tert-GO, SnO_2/GO and SnO_2 at different applied potentials. During 1 h electrolysis, 0.1 M $KHCO_3$ aqueous solution electrolyte at the cathodic part was under continuously mild stir and bubbled with CO_2 at the speed of 20 ml min^{-1}.

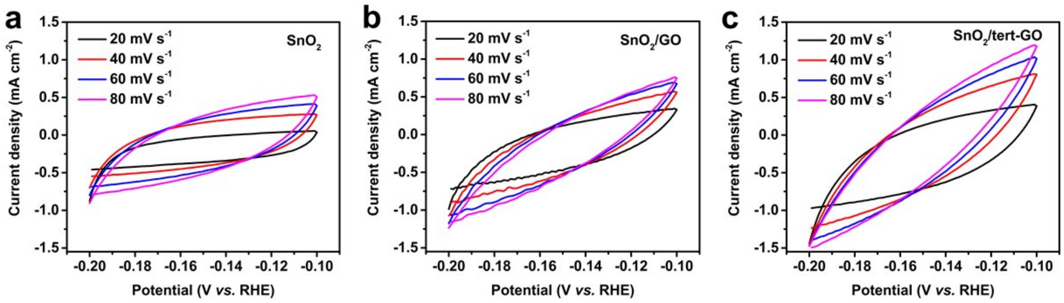

Figure S11. Cyclic voltammograms (CVs) of a) SnO_2/tert-GO, b) SnO_2/GO and c) SnO_2 between -0.2 V and -0.1 V vs. RHE in CO_2-saturated 0.1 M $KHCO_3$.

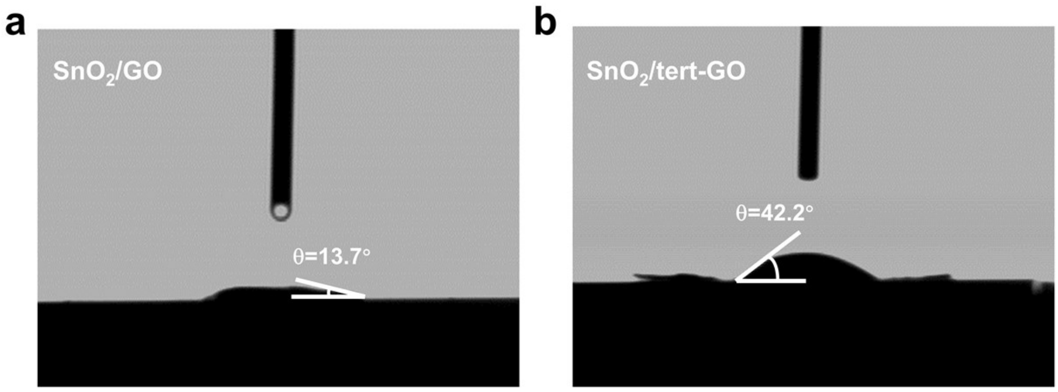

Figure S12. Contact Angle test diagrams of SnO_2/GO (a), and SnO_2/tert-GO (b).

Please do not adjust margins

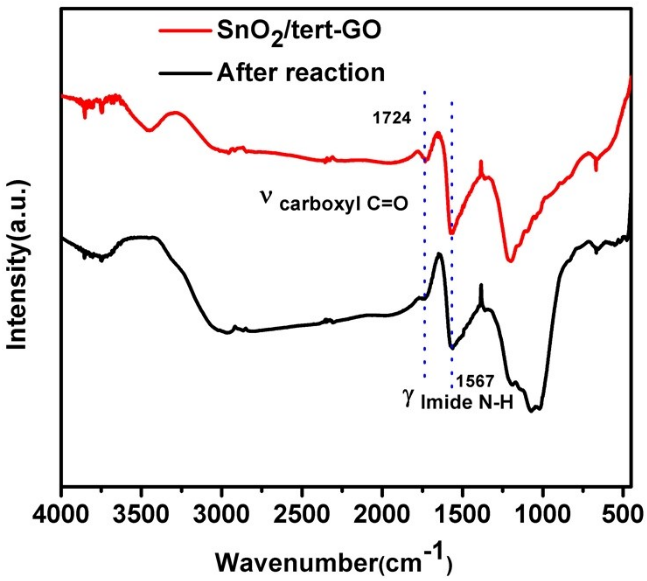

Figure S13. FTIR of SnO_2/tert-GO and SnO_2/tert-GO after reaction.

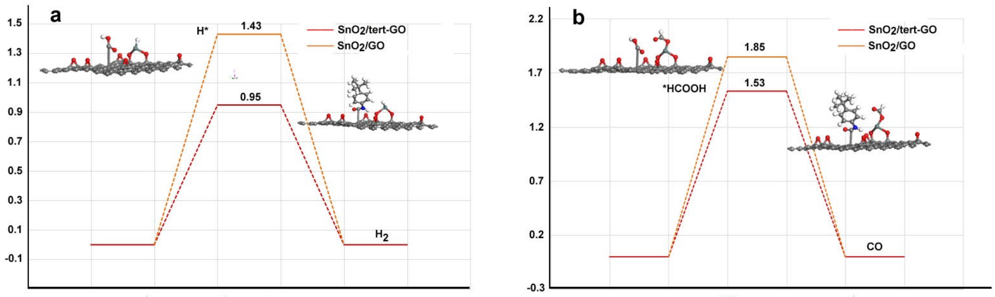

Figure S14. Theoretical calculation of conversion of CO_2 to CO and HER reaction

Table S1. Performance comparison of different metal–based electrocatalysts for CO_2 reduction to formate from recent literature.

Electrocatalysts	Electrolyte	Formate FE_{max}	j_{HCOO^-} at FE_{max}	Ref.
SnO_2-tert-GO	0.1 M $KHCO_3$	84.9 %@-0.96 V *vs.* RHE	3.7 mA cm^{-2}	**This work**
Sn/SnOx thin flm	0.5 M $NaHCO_3$	40%@-0.7 V *vs.* RHE	1.6 mA cm^{-2}	S1
Bi nanoflake	0.1 M $KHCO_3$	≈100%@-0.6 V *vs.* RHE	1.0 mA cm^{-2}	S2
Hierarchical Bi dendrite	0.5 M $KHCO_3$	≈89%@-0.74 V *vs.* RHE	2.4 mA cm^{-2}	S3
BiOx/C	0.5 M $NaHCO_3$	92.1%@−1.37 V *vs.* Ag/AgCl	1.35 mA cm^{-2}	S4
Sulfde-derived Bi	0.5 M $NaHCO_3$	84%@−0.75 V *vs.* RHE	4.2 mA cm^{-2}	S5
Sn-CF1000	0.1 M $KHCO_3$	62%@−0.8 V *vs.* RHE	11 mA cm^{-2}	S6
Nano-SnO_2/graphene	0.1 M $KHCO_3$	93.6%@−1.8 V *vs.* SCE	9.5 mA cm^{-2}	S7
SnO_2 pNWs	0.1 M $KHCO_3$	80%@−0.8 V *vs.* RHE	4.8 mA cm^{-2}	S8
Dendritic indium foams	0.5 M $KHCO_3$	86%@−0.86 V *vs.* RHE	5.0 mA cm^{-2}	S9

References

[S1] Y. Chen, M. W. Kanan, J. Am. Chem. Soc. 2012, 134, 1986.

[S2] S. Kim, W. J. Dong, S. Gim, W. Sohn, J. Y. Park, C. J. Yoo, H. W. Jang, J. L. Lee, Nano Energy 2017, 39, 44.

[S3] J. H. Koh, D. H. Won, T. Eom, N. K. Kim, K. D. Jung, H. Kim, Y. J. Hwang, B. K. Min, ACS Catal. 2017, 7, 5071.

[S4] C. W. Lee, J. S. Hong, K. D. Yang, K. Jin, J. H. Lee, H. Y. Ahn, H. Seo, N. E. Sung, K. T. Nam, ACS Catal. 2018, 8, 931.

[S5] Y. Zhang, F. Li, X. Zhang, T. Williams, C. D. Easton, A. M. Bond, J. Zhang, J. Mater. Chem. A 2018, 6, 4714.

[S6] Y. Zhao, J. Liang, C. Wang, J. Ma, G. G. Wallace, Adv. Energy Mater. 2018, 8, 1702524.

[S7] S. Zhang, P. Kang, T. J. Meyer, J. Am. Chem. Soc. 2014, 136, 1734.

[S8] B. Kumar, V. Atla, J. P. Brian, S. Kumari, T. Q. Nguyen, M. Sunkara, J. M. Spurgeon, Angew. Chem., Int. Ed. 2017, 56, 3645.

[S9] Z. Xia, M. Freeman, D. Zhang, B. Yang, L. Lei, Z. Li, Y. Hou, ChemElectroChem 2018, 5, 253.